Acta Crystallographica Section F
Structural Biology and Crystallization Communications
ISSN 1744-3091

Crystallization and preliminary X-ray diffraction analysis of human cytosolic seryl-tRNA synthetase

Jean-Baptiste Artero,[a,b,c] Susana C. M. Teixeira,[a,b,c] Edward P. Mitchell,[a,c,d] Michael A. Kron,[e] V. Trevor Forsyth[a,b,c] and Michael Haertlein[b,c]*

[a]EPSAM and ISTM, Keele University, Staffordshire ST5 5BG, England, [b]Institut Laue–Langevin, 6 Rue Jules Horowitz, 38042 Grenoble, France, [c]Partnership for Structural Biology, 6 Rue Jules Horowitz, 38042 Grenoble, France, [d]ESRF, 6 Rue Jules Horowitz, 38042 Grenoble, France, and [e]Department of Medicine, Biotechnology and Bioengineering Center, Medical College of Wisconsin, Milwaukee, Wisconsin 53226, USA

Correspondence e-mail: haertlein@ill.eu

Received 31 May 2010
Accepted 17 September 2010

Human cytosolic seryl-tRNA synthetase (hsSerRS) is responsible for the covalent attachment of serine to its cognate $tRNA^{Ser}$. Significant differences between the amino-acid sequences of eukaryotic, prokaryotic and archaebacterial SerRSs indicate that the domain composition of hsSerRS differs from that of its eubacterial and archaebacterial analogues. As a consequence of an N-terminal insertion and a C-terminal extra-sequence, the binding mode of $tRNA^{Ser}$ to hsSerRS is expected to differ from that in prokaryotes. Recombinant hsSerRS protein was purified to homogeneity and crystallized. Diffraction data were collected to 3.13 Å resolution. The structure of hsSerRS has been solved by the molecular-replacement method.

1. Introduction

The fidelity of protein biosynthesis is maintained by the specific attachment of amino acids to their cognate tRNA species. This process is catalyzed by a family of enzymes, the aminoacyl-tRNA synthetases (aaRSs), which discriminate with remarkable selectivity amongst many structurally similar tRNAs and amino acids. Sequence alignments (Eriani *et al.*, 1990; Cusack *et al.*, 1991) and structural analysis (Cusack *et al.*, 1990) have shown that the aaRS sequences are divided into two distinct classes. Seryl-tRNA synthetase, a member of class II, is an unusual enzyme compared with the other synthetases because of its substrate specificity. SerRS not only serylates $tRNA^{Ser}$ isoacceptors, but also the selenocysteine-incorporating $tRNA^{Sec}$. These tRNAs differ in sequence and structure, but share one structural element, a distinctive stem–loop structure located between the anticodon stem and the T stem called the long extra arm. $tRNA^{Ser}$ and $tRNA^{Sec}$ both fold into an L-shape, with the long extra arm uncoupled from the rest of the molecule (Dock-Bregeon *et al.*, 1990; Itoh *et al.*, 2009). The anticodon sequence is not required for aminoacylation specificity. Eukaryotic $tRNA^{Sec}$ is unique among all known tRNAs in having a long acceptor stem composed of nine base pairs (Sturchler *et al.*, 1993). Different recognition modes between SerRS and $tRNA^{Ser}$ exist in different kingdoms of life (Geslain *et al.*, 2006). The crucial role of the discriminator base has been documented for the human system (Breitschopf & Gross, 1996), together with the importance of the orientation and size, but not the sequence, of the variable loop (Heckl *et al.*, 1998). In bacteria, the charging of $tRNA^{Ser}$ depends on the recognition of some bases in the acceptor stem and the variable loop (Cusack *et al.*, 1996).

In contrast to vertebrate or other eukaryotic systems, prokaryotic SerRS systems have been extensively studied by X-ray crystallography. The X-ray structures of SerRS from *Escherichia coli* (Cusack *et al.*, 1990) and *Thermus thermophilus* (Fujinaga *et al.*, 1993) were found to be similar. The crystal structures revealed an N-terminal coiled-coil domain of about 90 residues that is flexibly attached and is called the helical arm and a catalytic domain comprising a seven-stranded antiparallel β-sheet with two connecting helices. The crystal structure of the complex between *T. thermophilus* SerRS and $tRNA^{Ser}$ revealed cross-subunit binding of the tRNA, an absence of protein interaction with the anticodon stem–loop and the importance of the interactions between the tRNA and the N-terminal helical arm

(Biou *et al.*, 1994; Cusack *et al.*, 1996). The functional importance of the coiled-coil arm in tRNA recognition has been demonstrated for bacterial enzymes (Borel *et al.*, 1994; Vincent *et al.*, 1995).

Methanogenic archaea possess unusual SerRSs that are evolutionarily distinct from those found in other archaea, eukaryotes and bacteria (Bilokapic *et al.*, 2006). The two types of SerRSs show only minimal sequence similarity, primarily within class II conserved motifs. SerRS represents the only known aminoacyl-tRNA synthetase system that has evolved two distinct mechanisms for the recognition of the same amino-acid substrate.

Similarly to other class II enzymes, bacterial, yeast cytosolic and vertebrate SerRSs are dimers. Eukaryotic aaRSs often contain N-terminal extensions, but only eukaryotic SerRS and IleRS possess C-terminal extra-domains (Weygand-Durašević *et al.*, 1996). It has been shown that the truncation of the C-terminal lysine-rich extension in yeast SerRS affects the stability and affinity of the enzyme for its substrates. The reason for an even longer extension in mammalian SerRS remains unclear. From sequence alignment, it is evident that human SerRS possesses an insertion of about 20 amino acids in the N-terminal domain in comparison with the prokaryotic, low eukaryotic and plant enzymes. The central part of this insertion is predicted to be α-helical (Raghava, 2000). A homologous metazoan/trypanosomatid-specific insertion into SerRS helix 2 has been identified by Geslain *et al.* (2006). The importance of this insertion requires further studies in order to determine its possible implication in tRNA binding or aminoacylation activity. Several class II human aaRSs have been shown to act as autoantigens in idiopathic inflammatory diseases of skeletal muscles (Plotz, 2002). In contrast to human AsnRS, which chemoattracts CCR3-transfected cells and immature dendritic cells (iDCs), which naturally produce CCR3, human SerRS *in vitro* chemoattracts CCR3-transfected HEK cells but not human iDCs (Howard *et al.*, 2002). Very recently, evidence has been provided for a noncanonical function of zebrafish SerRS in vascular development (Fukui *et al.*, 2009; Herzog *et al.*, 2009).

No crystallographic structure of any eukaryotic SerRS is available to date to allow structural insights into canonical and noncanonical functions. Here, we report the overproduction, crystallization and preliminary X-ray diffraction analysis of human SerRS.

2. Materials and methods

2.1. Overproduction and purification

The coding sequence of human cytosolic seryl-tRNA synthetase (hsSerRS; Vincent *et al.*, 1997; GenBank Accession No. BC000716.1) was cloned into pET28a expression vector (Novagen Inc.). The hsSerRS cDNA was inserted between *Nde*I and *Eco*I restriction sites (New England Biolabs). The resulting construct, which was verified by DNA sequencing, codes for hsSerRS with an N-terminal polyhistidine tag as a result of the cloning strategy. *E. coli* BL21 (DE3) cells were transformed with this construct and cultured in 1 l Luria–Bertani (LB) medium supplemented with 35 µg ml^{-1} kanamycin at 310 K until the OD_{600} reached 0.6. Protein overproduction was induced for 20 h at 293 K by adding isopropyl β-D-1-thiogalactopyranoside (IPTG) to a final concentration of 0.5 m*M*. Cells were harvested by centrifugation at 7330*g* for 20 min and resuspended in cold lysis buffer (20 m*M* Tris–HCl pH 7.9, 100 m*M* NaCl, 10 m*M* $MgCl_2$, 10% glycerol). Following cell lysis by sonication on ice, the cell extract was clarified by centrifugation at 29 000*g* for 45 min at 277 K. Imidazole (5 m*M*) and β-mercaptoethanol (3 m*M*) were added to the lysate. The supernatant solution was applied onto a nickel-chelating column (Ni–NTA Superflow, Qiagen) connected to an ÄKTAprime purification system (GE Healthcare) and pre-equilibrated with 20 m*M* Tris–HCl pH 7.9, 100 m*M* NaCl, 10 m*M* $MgCl_2$, 5 m*M* imidazole, 3 m*M* β-mercaptoethanol, 10% glycerol. To remove nucleic acids bound to hsSerRS, the column was first extensively washed with lysis buffer containing 1 *M* NaCl until the optical absorbance at 260 nm was stable. The column was then washed with lysis buffer containing 50 m*M* imidazole to remove remaining protein impurities. The synthetase was finally eluted with 20 m*M* Tris–HCl pH 7.9, 100 m*M* NaCl, 10 m*M* $MgCl_2$, 250 m*M* imidazole, 3 m*M* β-mercaptoethanol, 5% glycerol. After overnight dialysis against 20 m*M* Tris–HCl pH 7.9, 100 m*M* NaCl, 10 m*M* $MgCl_2$, 5% glycerol, 5 m*M* DTT, the protein was loaded onto a Superdex 200 10/300 GL gel-filtration column (GE Healthcare) equilibrated with the same buffer. The eluate from the gel-filtration column roughly matched the expected molecular mass of the SerRS dimer. The recovered protein was concentrated to 10 mg ml^{-1} by centrifugal ultrafiltration (Millipore; 5 kDa cutoff) and stored at 193 K. The purity of the protein was greater than 95% as judged by SDS–PAGE analysis (Fig. 1).

2.2. Crystallization and data collection

Crystals of hsSerRS were obtained from a freshly prepared protein solution comprising 10 mg ml^{-1} purified protein, 5 m*M* ATP (sodium salt; Boehringer Mannheim) and 2 m*M* L-serine (Sigma) in the final purification buffer. The nonhydrolyzable analogue 5′-*O*-[*N*-(L-seryl)-sulfamoyl]adenosine was also tested for cocrystallization, but the analogue did not improve the diffraction quality of the crystals. Extensive preliminary crystallization trials were performed at the EMBL-PSB crystallization platform with a PixSys4200 robot (Cartesian). Sparse-matrix crystal screens (Crystal Screen, Crystal Screen 2, Crystal Screen Lite, Natrix, MembFac and PEG/Ion from Hampton Research and Classics Suite from Qiagen) were tested using the vapour-diffusion method with drops consisting of 0.1 µl protein solution and 0.1 µl reservoir solution equilibrated against 88 µl reservoir solution (Dimasi *et al.*, 2007). Greiner CrystalQuick crystallization plates were used for the initial automated screenings. In order to improve the crystal dimensions and diffraction quality, the pH, temperature, precipitant concentration and precipitant:protein volume ratio of the crystallization hits were optimized. Manual screenings were carried out in Greiner Cryschem plates. The optimal crystallization drop volume was found to be 25 µl: slower crystallization and crystal-growth rates produced the largest best diffracting crystals.

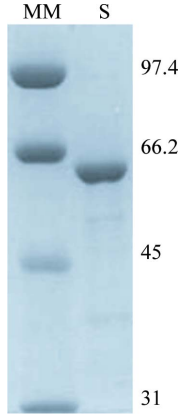

Figure 1
SDS–PAGE of hsSerRS. Lane MM, low-range molecular-mass markers from Bio-Rad; lane S, hsSerRS fraction from the Superdex 200 column.

Prior to data collection, a single crystal was soaked in a cryoprotectant solution composed of crystallization buffer supplemented with 20%(*v*/*v*) glycerol. Cryocooling was performed directly in a nitrogen stream at 100 K on the ID23-2 beamline at the ESRF (Grenoble, France). The beam energy was 14.20 keV (λ = 0.873 Å). A data set consisting of 130 images was collected to a maximum resolution of beyond 3.13 Å using a 1° oscillation step and a CCD detector (MAR Mosaic 225). Data were processed and scaled with *MOSFLM* (Leslie, 1992) and *SCALA* (Collaborative Computational Project, Number 4, 1994).

3. Results and discussion

The hsSerRS protein crystallized 8 d after initial setup using the sitting-drop vapour-diffusion method at 285 K. Crystals were obtained using a reservoir solution containing 100 m*M* ammonium sulfate, 22%(*w*/*v*) PEG 3350, 5% glycerol, 200 m*M* sodium formate pH 7.2. Briefly, 18.75 µl hsSerRS protein (10 mg ml^{-1} in 20 m*M* Tris–HCl pH 7.9, 100 m*M* NaCl, 10 m*M* $MgCl_2$, 5% glycerol, 5 m*M* DTT) and 6.25 µl reservoir solution were mixed and equilibrated against 500 µl reservoir solution. The hsSerRS crystals grew to maximum dimensions of 1.8 × 0.3 × 0.07 mm in two weeks (Fig. 2). Although the hsSerRS crystals appeared to grow with holes at the ends, they were suitable for X-ray diffraction experiments and a complete 3.13 Å resolution data set was collected (Fig. 3, Table 1). The data-set processing statistics revealed that the hsSerRS crystal had an orthorhombic lattice, with unit-cell parameters *a* = 116.1, *b* = 163.6, *c* = 172.5 Å and with systematic absences that were consistent with space group $P2_12_12_1$. Data-scaling statistics showed no evidence of crystal twinning. Although initial analysis of the crystal solvent using the Matthews coefficient (Matthews, 1968) suggested that the asymmetric unit contained three dimers of the hsSerRS protein with a solvent content of 46.01%, four molecules (two dimers) were finally found to be present. The self-rotation function indicated the presence of a tetrameric assembly. The human seryl-tRNA synthetase structure was solved by the molecular-replacement method with *Trypanosoma brucei* seryl-tRNA synthetase as the starting model (PDB code 3lsq; E. T. Larson, L. Zhang, A. Napuli, N. Mueller, C. L. M. J. Verlinde, W. C. Van Voorhis, F. S. Buckner, E. Fan, W. G. J. Hol & E. A. Merritt, unpublished work) using *Phaser* (McCoy *et al.*, 2007) as implemented in the *CCP*4 suite (Collaborative Computational Project, Number 4, 1994). The *Z* factor from *Phaser* was 21.3, indicating successful molecular replacement. The structure showed significant similarities to prokaryotic SerRS proteins in the catalytic core domain, but less so for the N-terminal helical arm region of the structure. Further model building and refinement is under way. Full details of this structure will be published elsewhere.

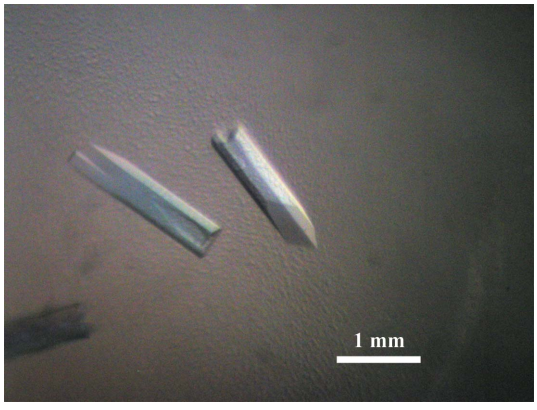

Figure 2
Single crystals of human seryl-tRNA synthetase.

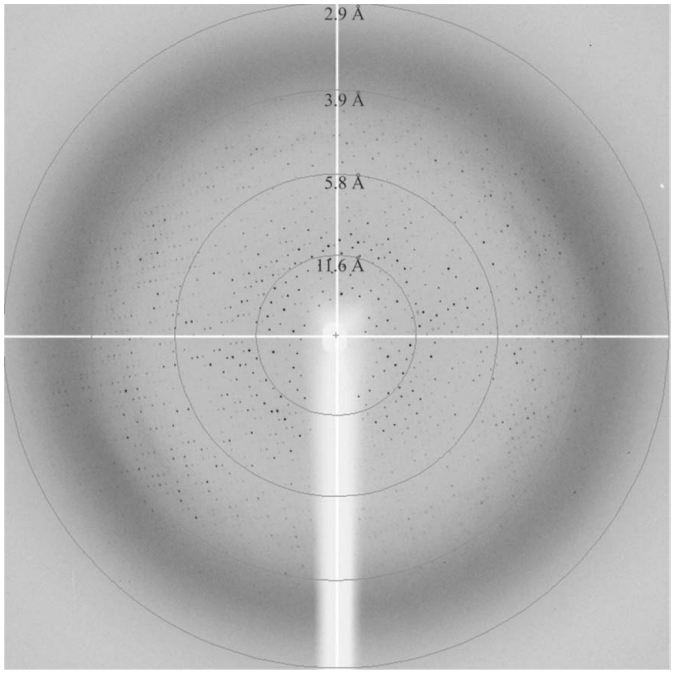

Figure 3
Diffraction pattern of a human seryl-tRNA synthetase protein crystal.

Table 1
X-ray data-collection and processing statistics.

Space group	$P2_12_12_1$
Unit-cell parameters (Å, °)	*a* = 116.1, *b* = 163.6, *c* = 172.5, α = β = γ = 90
Resolution (Å)	43.6–3.13 (3.30–3.13)
Unique reflections	58393 (8349)
Multiplicity	4.4 (4.1)
Completeness (%)	99.6 (99.0)
Average $I/\sigma(I)$	10.3 (2.0)
R_{merge}† (%)	0.114 (0.598)
No. of molecules in unit cell (*Z*)	4
Solvent content (%)	64.01

† $R_{merge} = \sum_{hkl}\sum_i |I_i(hkl) - \langle I(hkl)\rangle| / \sum_{hkl}\sum_i I_i(hkl)$, where $I_i(hkl)$ is the intensity of the *i*th observation of reflection *hkl* and $\langle I(hkl)\rangle$ is the weighted average intensity of *i* observations of reflection *hkl*.

The authors acknowledge the Engineering and Physical Sciences Research Council (EPSRC) for support under grants GR/R47950/01, GR/R99393/01 and EP/C015452/1. This work also benefited from activities associated with EU project funding under contracts 226507-NMI3, STRP-033256 and RII3-CT-2003-505925. Work by MK was supported in part by a cooperative agreement from the US National Institutes of Health (AI053877). We acknowledge Keele University for the support of SCMT as a Keele/ILL joint appointee. We thank the HT crystallization platform at the PSB for support, the ESRF for beam time and the staff of the Deuteration Laboratory for useful discussions.

References

Bilokapic, S., Maier, T., Ahel, D., Gruic-Sovulj, I., Söll, D., Weygand-Durasevic, I. & Ban, N. (2006). *EMBO J.* **25**, 2498–2509.
Biou, V., Yaremchuk, A., Tukalo, M. & Cusack, S. (1994). *Science*, **263**, 1404–1410.

Borel, F., Vincent, C., Leberman, R. & Hartlein, M. (1994). *Nucleic Acids Res.* **22**, 2963–2969.
Breitschopf, K. & Gross, H. J. (1996). *Nucleic Acids Res.* **24**, 405–410.
Collaborative Computational Project, Number 4 (1994). *Acta Cryst.* D**50**, 760–763.
Cusack, S., Berthet-Colominas, C., Hartlein, M., Nassar, N. & Leberman, R. (1990). *Nature (London)*, **347**, 249–255.
Cusack, S., Hartlein, M. & Leberman, R. (1991). *Nucleic Acids Res.* **19**, 3489–3498.
Cusack, S., Yaremchuk, A. & Tukalo, M. (1996). *EMBO J.* **15**, 2834–2842.
Dimasi, N., Flot, D., Dupeux, F. & Márquez, J. A. (2007). *Acta Cryst.* F**63**, 204–208.
Dock-Bregeon, A. C., Garcia, A., Giegé, R. & Moras, D. (1990). *Eur. J. Biochem.* **188**, 283–290.
Eriani, G., Delarue, M., Poch, O., Gangloff, J. & Moras, D. (1990). *Nature (London)*, **347**, 203–206.
Fujinaga, M., Berthet-Colominas, C., Yaremchuk, A. D., Tukalo, M. A. & Cusack, S. (1993). *J. Mol. Biol.* **234**, 222–233.
Fukui, H., Hanaoka, R. & Kawahara, A. (2009). *Circ. Res.* **104**, 1253–1259.
Geslain, R., Aeby, E., Guitart, T., Jones, T. E., Castro de Moura, M., Charrière, F., Schneider, A. & Ribas de Pouplana, L. (2006). *J. Biol. Chem.* **281**, 38217–38225.
Heckl, M., Busch, K. & Gross, H. J. (1998). *FEBS Lett.* **427**, 315–319.
Herzog, W., Müller, K., Huisken, J. & Stainier, D. Y. (2009). *Circ. Res.* **104**, 1260–1266.
Howard, O. M., Dong, H. F., Yang, D., Raben, N., Nagaraju, K., Rosen, A., Casciola-Rosen, L., Hartlein, M., Kron, M., Yang, D., Yiadom, K., Dwivedi, S., Plotz, P. H. & Oppenheim, J. J. (2002). *J. Exp. Med.* **196**, 781–791.
Itoh, Y., Chiba, S., Sekine, S. & Yokoyama, S. (2009). *Nucleic Acids Res.* **37**, 6259–6268.
Leslie, A. G. W. (1992). *Jnt CCP4/ESF–EACBM Newsl. Protein Crystallogr.* **26**.
Matthews, B. W. (1968). *J. Mol. Biol.* **33**, 491–497.
McCoy, A. J., Grosse-Kunstleve, R. W., Adams, P. D., Winn, M. D., Storoni, L. C. & Read, R. J. (2007). *J. Appl. Cryst.* **40**, 658–674.
Plotz, P. H. (2002). *Nature Rev. Immunol.* **3**, 73–78.
Raghava, G. P. S. (2000). *Protein Secondary Structure Prediction Using Nearest Neighbor and Neural Network Approach.* CASP4, 75–76. Protein Structure Prediction Center, University of California, Davis, USA.
Sturchler, C., Westhof, E., Carbon, P. & Krol, A. (1993). *Nucleic Acids Res.* **21**, 1073–1079.
Vincent, C., Borel, F., Willison, J. C., Leberman, R. & Hartlein, M. (1995). *Nucleic Acids Res.* **23**, 1113–1118.
Vincent, C., Tarbouriech, N. & Hartlein, M. (1997). *Eur. J. Biochem.* **250**, 77–84.
Weygand-Durašević, I., Lenhard, B., Filipić, S. & Söll, D. (1996). *J. Biol. Chem.* **271**, 2455–2461.